RECENT GAMS RESULTS ON MESON SPECTROSCOPY*

G. LANDSBERG

SUNY at Stony Brook, NY 11794–3800, USA

(for GAMS Collaboration)

D. Alde, F.G. Binon, C. Bricman, M. Boutemeur, S.V. Donskov, M. Gouanére, S. Inaba, A.V. Inyakin, V.A. Kachanov, G.V. Khaustov, E.A. Knapp, M. Kobayashi, A.A. Kondashov, A.V. Kulik, G.L. Landsberg, A.A. Lednev, V.A. Lishin, T. Nakamura, J.P. Peigneux, S.A. Polovnikov, V.A. Polyakov, M. Poulet, Yu.D. Prokoshkin, S.A. Sadovsky, V.D. Samoylenko, P.M. Shagin, A.V. Shtannikov, A.V. Singovsky, J.P. Stroot, V.P. Sugonyaev, K. Takamatsu, T. Tsuru

(Received July 23, 1993)

Recent results on $\omega\pi^0$ partial-wave analysis and model-independent measurements of rare $\omega \to \eta\gamma$ decay branching ratio from the GAMS Collaboration are presented. A partial-wave analysis of the 38 GeV/c data confirms the existence of the $\rho(2200)$ radial-orbital excitation of the $\rho(770)$ ground-state observed earlier in the same experiment. A new 5^{--} state, $\rho_5(2350)$, was also observed in this analysis. Masses, widths, and production cross sections for these states are given. The branching ratio for $\omega \to \eta\gamma$ decay was also measured and is compared with previous model-dependent measurements and with the predictions of a naive quark model. The measured value rules out the destructive ω-ρ interference, thus resolving ambiguity inherent to the earlier experiments.

PACS numbers: 14.40. Cs

---

* Presented at the Meson–Nucleus Interactions Conference, Cracow, Poland, May 14–19, 1993.

1. Introduction

The GAMS experiment [1] was launched in 1978 simultaneously at IHEP (Protvino) and at CERN (Geneva). The main goal of this experiment was a systematic study of the various meson systems decaying into all-gamma final states ($k\gamma$). The crucial part of the GAMS apparatus is a lead-glass Cherenkov electromagnetic calorimeter with energy resolution $\sigma_E/E \simeq 6\%/\sqrt{E\ [\mathrm{GeV}]} + 3\%$ and position resolution $\sigma_{X,Y} \simeq 6\ \mathrm{mm}/\sqrt{E\ [\mathrm{GeV}]}$ [2]. Such a fine calorimeter makes it possible to reconstruct the momenta of final state gamma quanta even for high multiplicity ($k \sim 10$), and thus to measure precisely the masses of the meson states decaying into a certain number of gammas. The matrix structure of the calorimeter allows one to reconstruct the topology of the final state without the ambiguities typical for planar hodoscopic devices.

The readout system [3] of the experiment consists of PMT's connected to the lead-glass blocks. The signals from the PMT are fed to 12-bit ADC's via 50 m signal cables. The readout electronics digitize the signals and subtract the pedestals. The data acquisition system [3] was originally based on a PDP 11/70 computer, which was later upgraded to μVAX II. Raw events were written on magnetic tape for further reconstruction by a standard program [4] and for physical analysis.

Historically, both the IHEP and CERN branches of the experiment were intended to study the charge-exchange reactions of the following type:

$$\begin{array}{l} \pi^- p \to M^0 n\,. \\ \qquad\quad \hookrightarrow \ldots \to k\gamma \end{array} \tag{1}$$

The IHEP experiment used a 38 GeV/c pion beam, while a 100 GeV/c pion beam was used at CERN. The layouts of the setups were similar [1], the only difference was in scale. The electromagnetic calorimeter at IHEP consisted of 1600 lead-glass blocks; the CERN calorimeter consisted of 4000 similar blocks. Reaction (1) was selected by a neutral trigger, organized by means of the scintillator/lead-glass guard system, surrounding a liquid hydrogen target. Scintillating counters were used to suppress any events with charge particles in the final state; lead-glass counters suppressed events with gamma quanta flying in the backward direction, thus ensuring a complete geometry for the experiment.

Later, both the IHEP and CERN experiments were upgraded in different ways. The IHEP branch got a wide-aperture lead/scintillator sampling electromagnetic calorimeter for studying high-spin resonances, and the CERN setup was modified for studying the central production reactions $((p,\pi)p \to (p,\pi)_f p_s M^0, M^0 \to k\gamma)$.

The results presented in this talk are based only on the 38 GeV/c charge-exchange $\pi^- p$ data taken in 1983, 1984 and 1987 runs at IHEP, when the two setups were still similar.

2. Partial-wave analysis of the $\omega\pi^0$ system at high masses

Recently, the analysis of the $\omega\pi^0$ system, produced in reaction (1) at 38 GeV/c and 100 GeV/c was completed. The $\pi^0\gamma$ decay mode of the ω meson, which corresponds to the 5γ final state of the $\omega\pi^0$ system, was studied. The first stage of this analysis which comprises mass spectrum analysis and a very simple pure-wave analysis was completed in 1989–1991 and the results have already been published [5]. The main result of this analysis was an observation along with the well-known $b_1(1235)$ and $\rho_3(1690)$ mesons, of a new state, $X/\rho(2200)$. It was shown that this state is produced via one-pion exchange (OPE), which restricts its quantum numbers to the following set: $J^{PC} = 1^{--}, 3^{--}, 5^{--} \ldots$; $I^G = 1^+$. A simplified wave analysis based on the assumption of pure non-interfering waves suggests quantum numbers 1^{--} for this state. Thus, we interpreted the $\rho(2200)$ meson as an orbital-radial excitation of $\rho(770)$ meson. The mass of this state is close to one expected from a simple Veneziano model [6] or from the Godfrey-Isgur model [7] for the $2\,^3D_1$ excitation. The new state was observed both at 38 GeV/c and at 100 GeV/c. The cross-sections of its production at both energies were measured. It was shown that the cross-section falls with energy quadratically as one expects for an OPE process (see [5] for details).

The second and the final stage of this analysis, which is the main subject of this talk, is a comprehensive mass-independent partial-wave analysis (PWA) of the $\omega\pi^0$ system at high masses and low momentum transfer.

Only the high-mass region, well above $b_1(1235)$, was used for this analysis in order to get rid of non-OPE processes. It was shown that at masses $M_{\omega\pi^0} \gtrsim 1.4$ GeV the number of events as a function of the upper $|t|$-cutoff, as well as angular distributions in the ω helicity frame, behave as one would expect for an OPE-dominated process. Thus, only events with $M_{\omega\pi^0} > 1.4$ GeV and $|t| < 0.1$ (GeV/c)^2 were used for the PWA. Other cuts and event selection procedures are the same as described in [5].

The 100 GeV/c CERN data was not used in this analysis, because the statistics accumulated at CERN were 10 times lower than that at IHEP.

2.1. Partial waves selection

The partial-wave analysis of high-mass and low-$|t|$ events was carried out under the assumption of OPE being dominant in these mass and momentum transfer regions of phase space. Both a simplified model without

absorption (pure OPE) and a poor-man's absorption model [8] were used to fit the experimental data.

The set of partial waves used in this analysis was restricted to 1^{--} 3^{--} and 5^{--} waves. Such a restricted set reflects the finite resolution of the GAMS detector at high $|\cos\vartheta_{GJ}|$ [1] which does not allow one to distinguish reliably between higher spins.

Only angular distributions in the Gottfried-Jackson frame were used for the partial-wave analysis.

2.2. Pure OPE partial-wave analysis formalism

First, the case of pure OPE, which means that only the ρ_{00} element of the density matrix not equal to 0, was considered. It can be shown straightforwardly, using the helicity formalism, that in this case the differential cross section for pure wave with spin J in the Gottfried-Jackson frame is as follows:

$$\frac{d^2\sigma^J}{d\cos\vartheta_{GJ}\,d\varphi_{TY}} \sim P_J^1(\cos\vartheta_{GJ})^2 . \tag{2}$$

Here $P_J^1(\cos\vartheta_{GJ})$ is an associated Legendre polynomial of degree J.

In case of several waves one should take interference into account. In the case of 3 waves expression (2) transforms into:

$$\frac{d^2\sigma}{dz\,d\varphi_{TY}} \sim |A_1 \cdot P_1^1(z) + A_3 \cdot P_3^1(z)e^{i\varphi_{31}} + A_5 \cdot P_5^1(z)e^{i\varphi_{51}}|^2 , \tag{3}$$

where $z \equiv \cos\vartheta_{GJ}$, A_J is a real amplitude of the wave J^{--}, and φ_{J1} is a real phase shift between waves J^{--} and 1^{--}. The overall phase of the 1^{--} wave can be chosen arbitrarily.

It is obvious from (3) that the cross section does not depend on the azimuthal angle in the Gottfried-Jackson frame. Experimental angular distributions in φ_{TY} in the described $(M_{\omega\pi^0}, t)$-region are consistent with this conclusion. Thus, it is sufficient to fit only one-dimensional differential cross section $d\sigma/dz$ in order to obtain amplitudes and phases of the partial waves.

It is trivial to show that (3) can be expanded in a set of regular Legendre polynomials of only even order:

$$\frac{d^2\sigma}{dz\,d\varphi_{TY}} \sim \frac{d\sigma}{dz} \sim a_0 \cdot P_0(z) + a_2 \cdot P_2(z) + \ldots + a_{10} \cdot P_{10}(z) , \tag{4}$$

---

[1] Here ϑ_{GJ} is a polar angle in the Gottfried-Jackson frame [9], which is a center-of-mass frame with Z-axis directed along beam particle momentum and with recoil particle momentum laying in the YZ-plane. The azimuthal angle in this frame is usually referred to as a Treyman-Yang angle φ_{TY}.

where $a_0, \ldots, a_{10}$ are some functions of the set $\mathcal{P} = \{A_1, A_3, A_5, \varphi_{31}, \varphi_{51}\}$.

It looks like the problem of determining the parameters $\mathcal{P}$ by fitting the experimental distributions could be solved very simply. Indeed, the experimental $\cos\vartheta_{GJ}$ distribution for a given $\omega\pi^0$-mass bin provides 6 even moments, which are basically equal to the coefficients a_i of the expansion (4). The number of unknown coefficients $\mathcal{P}$ is equal to 5 (3 real amplitudes and 2 real phases). Thus, the system of equations expressing 5 variables in terms of 6 measurables seems to be even overdetermined, so all 5 variables should be in principle unambiguously related with the moments of the angular distribution. However, it can be shown analytically that these 6 equations are in fact not independent of each other. Moreover, they are non-linear.

It was shown that in most of the cases such a non-linear system has two non-trivial solutions for the amplitudes A_1 and A_3. The highest amplitude A_5 is the same for both solutions (and this is the only variable which can be determined unambiguously). For each set of A_1, A_3, A_5 the two phases can be determined with a trivial ambiguity (which is just a sign of one of the phases). Thus, in most of the cases (which means in most of the mass bins) there exists a two-fold non-trivial ambiguity of the PWA solution.

2.3. Fitting procedure

In order to find both PWA solutions and to determine statistical errors of the parameters $\mathcal{P}$, a combination of analytical and numerical methods was used.

First, the mass spectrum of the $\omega\pi^0$ system was subdivided into a set of 50 MeV wide bins. For each mass bin, an *uncorrected* angular distribution in the Gottfried-Jackson angle ($dN/d\cos\vartheta_{GJ}$) was built and stored in the form of a histogram with the bin width of 0.1, which is on one hand broad enough to have a significant number of events in most of the bins, and on the other hand narrow enough to have a significant number of bins in such a histogram.

For each mass bin, the efficiency of the apparatus and of the physical cuts as a function of $\cos\vartheta_{GJ}$ was calculated using an event-by-event method. OPE distributions in all other variables were assumed during a Monte-Carlo calculation of the efficiency. The obtained efficiency as a function of the $\cos\vartheta_{GJ}$ was stored in a form of a histogram with the same bin width as for the histogram with the experimental angular distribution.

The set of variables $\mathcal{P}$ for each mass bin was determined by fitting the experimental histogram with the theoretical distribution (3) convoluted with the efficiency function. A maximum likelihood method was used for fitting. A Poisson distribution of the number of events per bin for the experimental data was assumed. Adjacent bins of the angular distribution

histogram were assumed to be non-correlated, which is a reasonable approximation since the width of the bin is in general much larger than the detector resolution in $\cos\vartheta_{GJ}$.

The likelihood function to be optimized has the following form:

$$L = \sum_{i=1}^{N_{\text{bin}}} \{\log(f(\mathcal{P})_i) \cdot \varepsilon_i - n_i\}. \tag{5}$$

Here N_{bin} equals to the number of bins in the experimental histogram ($N_{\text{bin}} = 20$), $f(\mathcal{P})_i$ is the expected number of events in i-th bin for given set $\mathcal{P}$ (f_i is defined by (3)), ε_i is the efficiency in i-th $\cos\vartheta_{GJ}$-bin, and n_i is the experimental number of events in i-th bin. The numerical minimization program MINUIT [10] was used for the optimization. MINUIT optimization ends up in one of the two equivalent maxima of the likelihood function, which gives the parameters of one of the two solutions with their correct errors. In order to find the other solution it was first calculated analytically using the parameters of the first one. Then MINUIT was used to perform a statistically correct optimization with an analytical solution parameters being used as a starting point close to the second maximum. Such a combination of analytical and numerical methods guarantees convergence of the optimization process and gives correct values and errors of the parameters $\mathcal{P}$ for both solutions.

The above procedure was applied in each $\omega\pi^0$-mass bin. As a result, both solutions were determined in each mass bin, and mass dependence of the partial amplitudes and the phases for both solutions was found.

The physically correct solution was selected by requiring a dominance of the $\rho_3(1690)$ peak in the amplitude squared of the 3^{--} wave. The existence of this peak and its quantum numbers were determined by different experiments in different decay modes of ρ_3, so the $\rho_3(1690)$ meson can be used as a reliable tool to distinguish between physical and unphysical solutions.

In order to describe the data below 1.4 GeV, a non-interfering S-wave was introduced. It has the parameters of $b_1(1235)$ meson and was normalized to its production cross-section [5] at $|t| < 0.1$ (GeV/c)^2. It proved to be a reasonable approximation for describing a low-mass region. Such a wave virtually does not affect the main PWA region $M_{\omega\pi^0} > 1.4$ GeV.

2.4. Pure OPE partial waves

The normalized 3^{--} amplitude squared for the physical solution is plotted in Fig. 1. The $\rho_3(1690)$ peak indeed dominates the spectrum. A fit with a sum of Breit-Wigner curve and a polynomial background gives the following parameters of this resonance:

$$M(\rho_3) = 1669 \pm 25 \text{ MeV},$$
$$\Gamma(\rho_3) = 230 \pm 65 \text{ MeV},$$
$$\sigma(\pi^- p \to \rho_3 n) \cdot BR(\rho_3 \to \omega\pi^0) = 1.13 \pm 0.20 \ \mu\text{b}. \quad (6)$$

The mass and the width are consistent with PDG data [11]. The cross section data agrees with our previous result obtained from the mass-spectrum analysis [5]. Here and in what follows the cross-section was calculated for the whole t-range, and the OPE t-dependence [5] was used for these calculations.

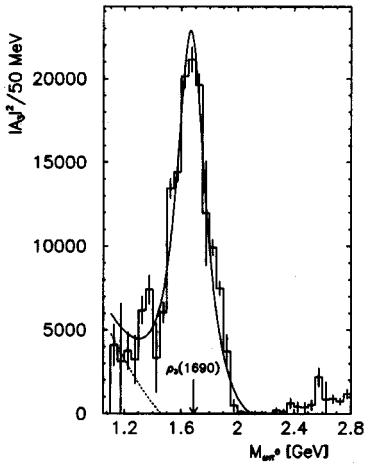

Fig. 1. Amplitude squared of the 3^{--} wave. Histogram shows the PWA results; solid curve — results of the fit with a sum of Breit-Wigner resonance and a polynomial background (dashed curve). Arrow indicates the $\rho_3(1690)$ meson mass.

The normalized 1^{--} amplitude squared for the physical solution is shown in Fig. 2. The main structure observed in the spectrum is a broad $\rho(2200)$ meson with the following parameters:

$$M(\rho) = 2140 \pm 30\text{MeV},$$
$$\Gamma(\rho) = 320 \pm 70\text{MeV},$$
$$\sigma(\pi^- p \to \rho n) \cdot BR(\rho \to \omega\pi^0) = 250 \pm 60 \ n\text{b}. \quad (7)$$

These parameters are close to our preliminary results [5], except for the cross-section which was underestimated in the preliminary analysis due to an incorrect background parametrization. Current PWA shows that most of the "background" in the $\omega\pi^0$ mass spectrum is in fact a result of the

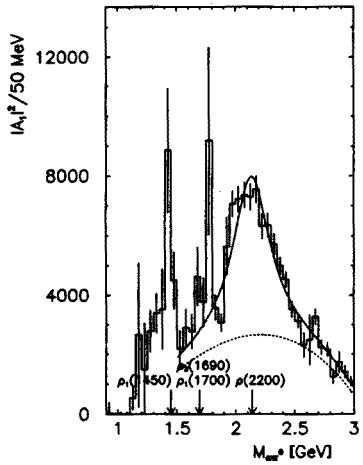

Fig. 2. Amplitude squared of the 1^{--} wave. Histogram shows the PWA results; solid curve — results of the fit with a sum of Breit-Wigner resonance and a polynomial background (dashed curve). Arrows indicate the masses of $\rho(1450)$, $\rho_3(1690)$, $\rho(1700)$ and $\rho(2200)$ mesons.

interference between ρ_3 and $\rho(2200)$, so it must be taken into account when calculating the cross-section.

The last result confirms the observation of the radial-orbital excitation of the $\rho(770)$ meson claimed in our previous work [5]. The $\rho(2200)$ meson is the only statistically significant structure in 1^{--} wave spectrum. A spike at 1.7 GeV is most likely explained by a leakage from a 3^{--} wave to a 1^{--} wave due to the uncertainties of efficiency calculations, finite detector resolution in $\cos\vartheta_{GJ}$ etc. An analogous spike at 1.4 GeV might be due to the significant amount of non-OPE $b_1(1235)$ tail in that mass region. However, one should also expect some 1^{--} activity in these two regions due to $\rho_1(1450)$ and $\rho_1(1700)$ lower excitations of $\rho(770)$ meson [11].

Finally, the normalized 5^{--} amplitude squared is shown in Fig. 3. As has been mentioned, it is the same for both PWA solutions. The spectrum shows a statistically significant structure in the 2.4 GeV mass region. A fit with a sum of one Breit-Wigner curve and a polynomial background (see Fig. 3a) gives the following parameters for this structure which in what follows will be referred to as the $\rho_5(2350)$ meson:

$$\begin{aligned} M(\rho_5) &= 2330 \pm 35\text{MeV}, \\ \Gamma(\rho_5) &= 400 \pm 100\text{MeV}, \\ \sigma(\pi^- p \to \rho_5 n) \cdot BR(\rho_5 \to \omega\pi^0) &= 130 \pm 40\ \text{nb}. \end{aligned} \tag{8}$$

The mass of the new state is close to what one should expect from a simple Regge model for the 5^{--} ground-state. The evidences for existence

of the 5^{--} wave at 2.35 GeV were previously found in partial-wave analysis of the $\pi\pi$ data obtained in $p\bar{p}$ production and annihilation experiments [12]. Some activity in the 1.7 GeV mass region reflects a leakage from the 3^{--} wave dominated by a huge $\rho_3(1690)$ resonance.

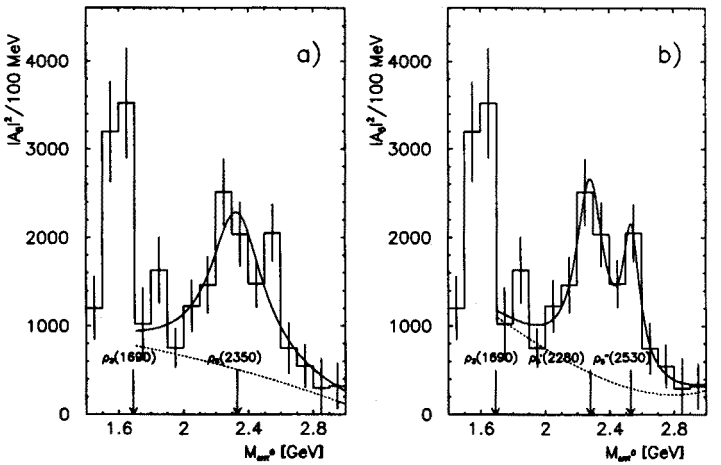

Fig. 3. Amplitude squared of the 5^{--} wave. Histograms show the PWA results. a) Solid curve — results of the fit with a sum of one Breit-Wigner resonance and polynomial background (dashed curve). b) Solid curve — results of the fit with a sum of two Breit-Wigner resonances and a polynomial background (dashed curve). Arrows indicate the masses of $\rho_3(1690)$, $\rho_5(2350)$, $\rho_5'(2280)$ and $\rho_5''(2550)$ mesons.

It is also possible to fit the data introducing two Breit-Wigner resonances (see Fig. 3b). In this case the $\rho_5(2350)$ state splits into two narrow resonances ρ_5' and ρ_5'' with the following masses and widths: 2280 ± 20 MeV, 180 ± 80 MeV and 2535 ± 35 MeV, 100 ± 60 MeV. Their production cross sections are 80 ± 30 nb and 40 ± 15 nb, respectively. The masses for the split resonances are in good agreement with what one should expect from a naive mass formula for $3\ ^5G$ and $3\ ^5I$ states [13]. However, one cannot claim the existence of two resonances because the statistical significance of this fit is approximately the same as for the one-resonance fit. Thus, in what follows, only one resonance in 5^{--} wave, $\rho_5(2350)$, will be discussed.

The behavior of the relative phases between 1^{--} and 3^{--} waves, as well as between 3^{--} and 5^{--} waves (Fig. 4a,b), shows two phase-flips near the resonance maxima, as one should expect for two distant resonances. The behavior of the relative phase between 1^{--} and 5^{--} waves is quite smooth, because both $\rho(2200)$ and $\rho_5(2350)$ are broad and significantly overlap in mass.

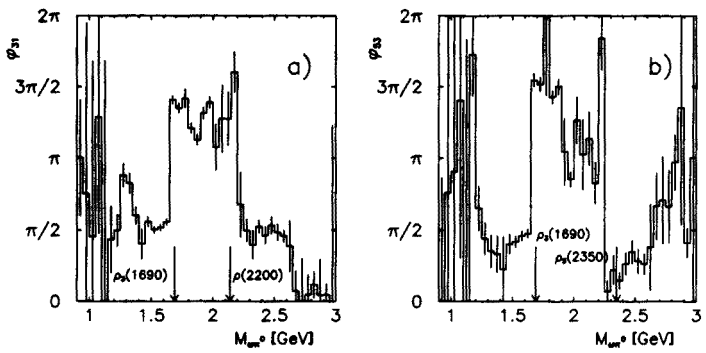

Fig. 4. a) Phase shift between 3^{--} and 1^{--} waves. b) Phase shift between 5^{--} and 3^{--} waves. Arrows indicate the masses of $\rho_3(1690)$, $\rho(2200)$ and $\rho_5(2350)$ mesons.

2.5. Partial-wave analysis for OPE with absorption

An attempt to perform the PWA for OPE with an additional absorption term was also made. The Ochs-Wagner modification of the poor-man's absorption model (PMA) [8] was used for this analysis. In this model, in the assumption of an S-channel nucleon spin-flip dominance, one expects additional φ_{TY}-dependent terms in the expansion of the differential cross section in Gottfried-Jackson frame. The expression (4) transforms into:

$$\frac{d^2\sigma}{dz\,d\varphi_{\mathrm{TY}}} \sim a_0 \cdot Y_0^0(z,\varphi_{\mathrm{TY}}) + a_2 \cdot Y_2^0(z,\varphi_{\mathrm{TY}}) + \ldots + a_{10} \cdot Y_{10}^0(z,\varphi_{\mathrm{TY}}) + b_2 \cdot Y_2^1(z,\varphi_{\mathrm{TY}}) + \ldots + b_{10} \cdot Y_{10}^1(z,\varphi_{\mathrm{TY}}). \tag{9}$$

Here, $Y_J^m(z,\varphi_{\mathrm{TY}})$ are spherical harmonics.

The Ochs-Wagner model also superimposes certain constraints on the amplitudes a_J and b_J. It could be shown that for $J \geq 2$

$$\frac{b_J}{a_J} \sim \frac{\sqrt{J(J+1)}}{M_{\omega\pi^0}}. \tag{10}$$

It is obvious from (10) that the main contribution of the absorption terms is observed for lower masses and higher spins. So, one should expect the largest distortion of the pure OPE results for $\rho_3(1690)$ (low mass and relatively high spin) and for $\rho_5(2350)$ (high mass, but very high spin), while for $\rho(2200)$ the correction must be small.

An analytical analysis of the non-linear equations relating amplitudes, phases and absorption parameter with 11 moments in formula (9) was not yet carried out. Instead of this the PWA equations with absorption were

solved only for the highest wave amplitude (5^{--}), which still can be determined unambiguously.

An extension of the technique described in 2.2 for 2-dimensional histograms with $(\cos\vartheta_{GJ}, \varphi_{TY})$ angular distribution was used in order to determine this amplitude in each mass bin.

It was shown that all odd moments of angular distributions are compatible with zero, as well as the moments for Y_J^m with $m \neq 0, 1$. It was also shown, that the experimental data follows prediction (10) rather well.

The structure at 2.35 GeV in the 5^{--} amplitude squared mass spectra survives after introduction of the absorption terms, and the parameters of its fit with either one or two Breit-Wigner resonances do not change within the errors, comparing with the pure OPE results (8). The contribution of the absorption terms in $\rho_5(2350)$ mass region was found to be about 10%. However, the quality of the maximum likelihood fit of the high-mass data (dominated by $\rho_5(2350)$ meson) improved significantly, and the corresponding χ^2 per degree of freedom drops from $\simeq 2$ to $\simeq 0.9$ with the absorption taken into account. The quantitative results on absorption corrections are in agreement with $\pi^- p \to \pi^+\pi^- n$ PWA at 100 GeV/c and 175 GeV/c [14]. Using the scale of absorption corrections for $\rho_5(2350)$ and formula (10), it is easy to show that the contribution of absorption terms in the $\rho(2200)$ meson region is less than 3%, and one can safely neglect it. The contribution of absorption terms in the ρ_3 meson region is about 9%, but this meson has been studied before in many other experiments, so there is no urgent need to improve the estimates (6) of its parameters by accounting for the absorption. Thus, it was decided not to perform further analytical analysis of the equations with absorption terms, because the pure OPE approximation seems to work well for the low-spin $\omega\pi^0$ data.

2.6. Summary of $\omega\pi^0$ PWA results

As a result of a thorough partial-wave analysis the existence of the $\rho(2200)$ meson was confirmed. A new 5^{--} state, $\rho_5(2350)$, not seen in the mass spectrum analysis, was also observed both within pure OPE and PMA OPE approximations. The parameters and the production cross sections for these resonances, as well as for $\rho_3(1690)$ meson were measured. The masses of $\rho(2200)$ and $\rho_5(2350)$ mesons are in a good agreement with Veneziano formula [6], Godfrey–Isgur model [7] and Regge model predictions, respectively. Comparison of these models with GAMS data and other experimental results is shown in Fig. 5a,b.

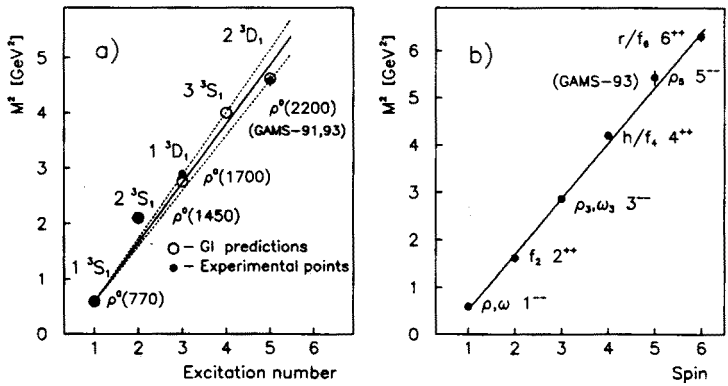

Fig. 5. a) Excitation trajectory for ρ mesons. Dots with the error bars show experimental data; open circles — Godfrey–Isgur predictions [7]; solid line and dashed lines — Veneziano formula predictions and its errors [6]. b) Regge trajectory for ρ, ω and f mesons. Dots with error bars show experimental data; solid line — least squares fit to the data.

3. Model-independent measurement of the $\omega \to \eta\gamma$ branching ratio

Another recent result obtained by the GAMS Collaboration is a model-independent measurement of the probability of the rare $\omega \to \eta\gamma$ decay. This decay was previously measured in e^+e^--annihilation [15] and photoproduction [16] experiments. The main problem of previous experiments was a strong dependence of the results on the exact value of ω-ρ mixing [17]. Under the assumption of a constructive ω-ρ interference (favored by quark model) the following, model-dependent, branching ratio was obtained [11]:

$$BR(\omega \to \eta\gamma) = (5 \pm 2) \times 10^{-4}. \tag{11}$$

Studying of the charge exchange reaction

$$\begin{aligned} \pi^- p &\to \omega\, n \\ &\hookrightarrow \eta\gamma \to 3\gamma \end{aligned} \tag{12}$$

allows one to determine the branching ratio (11) model-independently, because the contribution of the ω-ρ interference which occurs due to the corresponding reaction with ρ meson:

$$\pi^- p \to \rho^0\, n, \tag{13}$$

can been effectively suppressed by a t-cut. Indeed, the production of ω in (12) is dominated by natural parity exchange, while the production of ρ^0 in the reaction (13) is dominated by OPE, which falls down rapidly with $|t|$.

The 38 GeV/c data taken at IHEP with GAMS-2000 apparatus in 1984 was used for this analysis. The details of the event selection criteria and cuts are described in [18]. Only $|t| > 0.15$ $(\mathrm{GeV/c})^2$ data for which the ω-ρ interference correction has been shown to be less than 20% was used for the branching ratio calculations.

A thorough Monte-Carlo analysis of the combinatorial background was carried out. This background occurs due to the possible ambiguity of associating η meson with one of the three pair combinations of 3 gammas in the final state.

The raw mass spectrum of the $\eta\gamma$ system after subtraction of the combinatorial background is shown in Fig. 6a. A clear peak in the ω mass region, observed in this spectrum, corresponds to the rare decay (12). The same spectrum corrected for the detector acceptance and the efficiency of the cuts used during the analysis is shown in Fig 6b.

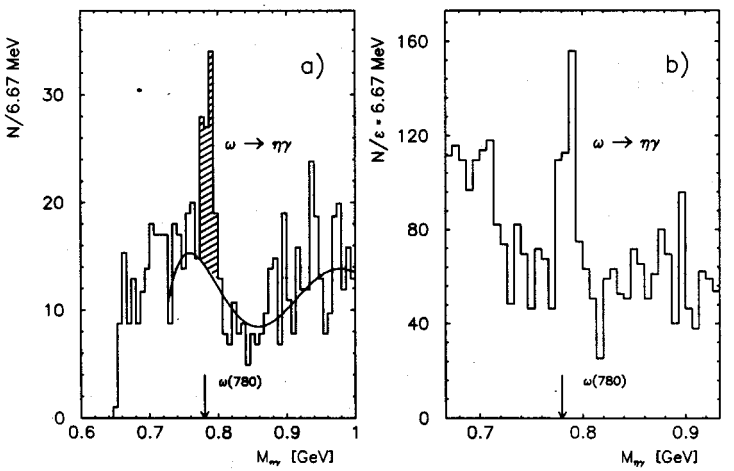

Fig. 6. a) Histogram shows raw mass spectrum of the $\eta\gamma$ system after subtraction of the combinatorial background; solid line — Monte-Carlo simulation of the background; hatched area corresponds to decay (12). b) Same spectrum corrected for the efficiency of the detector and physical cuts. Arrow indicates the ω meson mass.

Using the number of $\omega \to \pi^0\gamma$ decay events observed in the same charge-exchange reaction for normalization, the following model-independent branching ratio was obtained:

$$BR(\omega \to \eta\gamma) = (8.3 \pm 2.1) \times 10^{-4}\,. \qquad (14)$$

The error includes systematical uncertainties due to the residual ω-ρ interference. This result is close to the model-dependent PDG value (11) and to

the naive quark model predictions. It also resolves the ambiguity of earlier results [15, 16] due to the unknown sign of the ω-ρ interference. GAMS data rules out the destructive ω-ρ interference.

REFERENCES

[1] F. Binon *et al.*, *Nucl. Instr. Meth.* **A248**, 86 (1986); *Cherenkov Detectors and Their Applications in Science and Technics*, Nauka, Moscow 1990, p. 149.
[2] F. Binon *et al.*, *Nucl. Instr. Meth.* **A188**, 507 (1981).
[3] D. Alde *et al.*, *Nucl. Instr. Meth.* **A240**, 343 (1985).
[4] D. Alde *et al.*, *Phys. Lett.* **B182**, 105 (1986); *Pis'ma JETP* **44**, 441 (1986); *Nucl. Instr. Meth.* **A268**, 112 (1988); *Yad. Fiz.* **49**, 1021 (1989); *Phys. Lett.* **B216**, 451 (1989).
[5] G. Landsberg, Proc. 4th Int. Conf. on Hadron Spectroscopy HADRON '91, College Park, 1991, p. 13; D. Alde *et al.*, *Z. Phys.* **C54**, 553 (1992).
[6] G. Veneziano, *Nuovo Cimento* **57**, 190 (1968).
[7] S. Godfrey, N. Isgur, *Phys. Rev. Lett.* **D32**, 189 (1985).
[8] P.K. Williams, *Phys. Rev.* **D1**, 1312 (1970); W. Ochs, F. Wagner, *Phys. Lett.* **B44**, 271 (1973); F. Wagner, *Nucl. Phys.* **B58**, 494 (1973).
[9] J.D. Jackson, *Nuovo Cimento* **34**, 1645 (1964).
[10] F. James, M. Roos, preprint CERN–DD/75/20, Geneva 1975.
[11] Review of Particle Properties, Particle Data Group, *Phys. Rev.* **D4** 1992 VII.16, 44–45, 53–54, 57–58.
[12] B.R. Martin, D. Morgan, *Nucl. Phys.* **B176**, 355 (1980).
[13] D.C. Peaslee, private communication.
[14] S.R. Stampke, Ph.D. Thesis, CALT–68–936, Pasadena 1982.
[15] S.I. Dolinsky *et al.*, *Z. Phys.* **C42**, 511 (1989).
[16] D.E. Andrews *et al.*, *Phys. Rev. Lett.* **38**, 198 (1977).
[17] N.N. Achasov, G.N. Shestakov, *Elem. Part. Atom. Nucl.* **9**, 48 (1978).
[18] D. Alde *et al.*, preprint IHEP 93–29, Protvino 1993.